

# Dual-Energy CT in the Assessment of Mediastinal Lymph Nodes: Comparative Study of Virtual Non-Contrast and True Non-Contrast Images

Seon Young Yoo, MD<sup>1,3</sup>, Yookyung Kim, MD<sup>2</sup>, Hyun Hae Cho, MD<sup>2</sup>, Mi Joo Choi, MD<sup>2</sup>,  
Sung Shine Shim, MD<sup>2</sup>, Jeong Kyong Lee, MD<sup>2</sup>, Seung Yon Baek, MD<sup>2</sup>

<sup>1</sup>Department of Radiology, School of Medicine, Ewha Womans University, Seoul 158-710, Korea; <sup>2</sup>Department of Radiology, School of Medicine, Ewha Womans University, Mokdong Hospital, Seoul 158-710, Korea; <sup>3</sup>Department of Radiology, Kepeco Medical Center, Seoul 132-703, Korea

**Objective:** To evaluate the reliability of virtual non-contrast (VNC) images reconstructed from contrast-enhanced, dual-energy scans compared with true non-contrast (TNC) images in the assessment of high CT attenuation or calcification of mediastinal lymph nodes.

**Materials and Methods:** A total of 112 mediastinal nodes from 45 patients who underwent non-contrast and dual-energy contrast-enhanced scans were analyzed. Node attenuation in TNC and VNC images was compared both objectively, using computed tomography (CT) attenuation, and subjectively, via visual scoring (0, attenuation  $\leq$  the aorta; 1,  $>$  the aorta; 2, calcification). The relationship among attenuation difference between TNC and VNC images, CT attenuation in TNC images, and net contrast enhancement (NCE) was analyzed.

**Results:** CT attenuation in TNC and VNC images showed moderate agreement (intraclass correlation coefficient, 0.612). The mean absolute difference was  $7.8 \pm 7.6$  Hounsfield unit (HU) (range, 0-36 HU), and the absolute difference was equal to or less than 10 HU in 65.2% of cases (73/112). Visual scores in TNC and VNC images showed fair agreement ( $\kappa$  value, 0.335). Five of 16 nodes (31.3%) which showed score 1 ( $n = 15$ ) or 2 ( $n = 1$ ) in TNC images demonstrated score 1 in VNC images. The TNC-VNC attenuation difference showed a moderate positive correlation with CT attenuation in TNC images (partial correlation coefficient [PCC] adjusted by NCE: 0.455) and a weak negative correlation with NCE (PCC adjusted by CT attenuation in TNC: -0.245).

**Conclusion:** VNC images may be useful in the evaluation of mediastinal lymph nodes by providing additional information of high CT attenuation of nodes, although it is underestimated compared with TNC images.

**Index terms:** Dual-energy CT; Chest; Lymph nodes; Virtual non-contrast; Iodine subtraction

Received August 31, 2012; accepted after revision October 17, 2012.

**Corresponding author:** Yookyung Kim, MD, Department of Radiology, School of Medicine, Ewha Womans University, Mokdong Hospital, 1071 Anyangcheon-ro, Yangcheon-gu, Seoul 158-710, Korea.

• Tel: (822) 2650-5380 • Fax: (822) 2650-5302  
• E-mail: yookkim@ewha.ac.kr

This is an Open Access article distributed under the terms of the Creative Commons Attribution Non-Commercial License (<http://creativecommons.org/licenses/by-nc/3.0>) which permits unrestricted non-commercial use, distribution, and reproduction in any medium, provided the original work is properly cited.

## INTRODUCTION

In patients with non-small cell lung cancer (NSCLC), calcification or computed tomography (CT) attenuation higher than the great vessels on non-contrast images is one of the key diagnostic parameters of benignity in the assessment of mediastinal lymph nodes. The judicious use of this parameter may help to reduce the false positive rate in mediastinal nodal staging using fluorine-18-fluorodeoxyglucose positron emission tomography (FDG-PET) (1-6). However, although high attenuation or even

calcification may be obscured on contrast-enhanced images (7), non-contrast scans are not typically included in routine chest CT protocols because they increase the patient's radiation exposure.

The dual-energy CT technique allows differentiation of iodine from other materials due to its stronger photoelectric absorption. This feature enables the virtual 'subtraction' of the iodine content from a contrast-enhanced dual-energy CT scan, thereby providing a virtual non-contrast (VNC) image (8-10). If such VNC images could be reliably used to detect calcification or strongly attenuating nodes, additional non-contrast enhanced scanning may be prevented, and the patient's radiation exposure will then be reduced.

The purpose of this study was to evaluate the reliability of virtual non-contrast (VNC) images reconstructed from contrast-enhanced, dual-energy scans compared to true non-contrast (TNC) images in the assessment of high CT attenuation or calcification of mediastinal lymph nodes.

## MATERIALS AND METHODS

This study was approved by our institutional review board, which waived informed consent for the retrospective data analysis of dual-energy CT scans obtained for clinical purposes.

### Subjects

Images were obtained from 218 consecutive patients who underwent chest CT scans that included a single-energy non-contrast scan, followed by a post contrast dual-energy CT scan as part of their routine disease assessment from November 2010 to March 2011 in our tertiary hospital. All patient contrast-enhanced images were retrospectively reviewed by an experienced radiologist (SY Yoo; 18 year-experience of chest CT interpretation), and mediastinal nodes with a short axis diameter of  $\geq 1$  cm and no demonstrable calcification on contrast-enhanced images were enrolled for this study. Maximally, four nodes in each patient were included for analysis. CT scans from 45 patients with a total of 112 mediastinal nodes were enrolled in this study. A total of 21 male and 24 female patients were enrolled, with a mean age of  $63.7 \pm 12.7$  years (mean  $\pm$  standard deviation [SD]; range, 40-87 years).

A total of 173 patients were excluded from this study based on the exclusion criteria as follows: nodes of short axis less than 1 cm ( $n = 140$ ); nodes for which a usable TNC + VNC CT image set was not available due to beam

hardening or partial volume averaging artifacts ( $n = 13$ ) or a different level of CT scanning ( $n = 5$ ); and nodes showing calcification on contrast-enhanced images ( $n = 15$ ).

### Acquisition of CT Images

All CT scans were obtained in the supine position with a dual-source multi-detector row scanner (SOMATOM Definition Flash; Siemens Medical Solutions, Forchheim, Germany). The single-energy TNC scan was performed at a collimation of  $1 \times 128 \times 0.6$  mm, 120 kVp, 100 mAs (effective), a pitch of 1.2, and a gantry rotation time of 0.5 s, with on-line dose modulation (Care DOSE 4D; Siemens Medical Solutions, Erlangen, Germany) enabled.

The subsequent dual-energy contrast-enhanced scan was acquired with  $2 \times 32 \times 0.6$  mm collimation, a pitch of 0.55, a gantry rotation time of 0.28 s, and at 80 kVp/205 mAs (effective) (Tube A) and 140 kVp/87 mAs (effective) (Tube B). With both tubes, online dose modulation was used. The CT scan was obtained 40 s after intravenous injection of 100 mL of a nonionic contrast agent (iohexol, Bonorex 350; CMS, Seoul, Korea) at a rate of 2.3 mL/s with power injection.

All TNC and dual-energy contrast-enhanced scans were reconstructed in a transverse orientation at a slice thickness of 3 mm, using soft-tissue kernels (B30f).

The radiation doses of non-contrast and dual-energy CT scans were recorded as the value of the volume CT dose index (CTDI) and the dose-length product (DLP).

### Dual-Energy Image Reconstruction

For all 45 patients, dual-energy CT data were transferred to a workstation (Syngo Multi Modality Workplace [MMWP]; Siemens AG, Healthcare Sector, Forchheim, Germany) for further analysis. The dual-energy datasets were post-processed using clinically available dedicated software. The Liver VNC application class (Syngo, Dual Energy, Siemens Medical Solutions, Erlangen, Germany) was used to reconstruct transverse VNC images without changing slice thickness or reconstruction intervals. We used the default settings of Liver VNC, with nominal CT values for fat of -110 (-87) Hounsfield unit (HU) at low (high) tube voltage and 60 (55) HU for soft tissue at low (high) tube voltage. A relative contrast medium enhancement of 3.01 was used, meaning that the iodine enhancement at 80 kV is 3.01 times the value at 140 kV. The minimum cut-off was -300 HU, and the maximum cut-off was 3071 HU.

### Image Analysis

In the objective analysis, CT attenuation measurements were made by one investigator (SY Yoo). The TNC and VNC images of each patient were aligned next to each other. The region of interest (ROI) was delineated; the investigator attempted to include as great an area as possible but smaller than the size of node, thereby avoiding partial volume averaging. The size and location of the ROI was kept constant between the TNC and VNC series. CT attenuation was measured three times in each node, and the mean value was used for analysis.

In the subjective analysis, the lymph node was evaluated using the following three-point scoring system: score of 0, node attenuation is equal to or less than that of the aorta; score of 1, node attenuation is greater than that of the aorta; and score of 2, node shows calcification. These visual assessments were carried out independently by two experienced radiologists (Y Kim, SS Shim; 16 and 10 years of experience in interpreting chest CT images, respectively) with mediastinal window images (level, 400 H; width, 40 H). Each radiologist evaluated the series of VNC images first, and then evaluated TNC images while blinded to the results of the VNC image set. There was no discrepancy between two readers in the interpretation of TNC images. In two cases in which lymph nodes were interpreted as score 1 by reader 1 and score 0 by reader 2 on VNC images, the nodes were scored as 1 by consensus.

To assess factors potentially affecting CT attenuation in VNC images, the relationships among the TNC-VNC attenuation difference, CT attenuation in TNC images, and the net contrast enhancement were evaluated. For this analysis, CT attenuation of each node was measured in a series of contrast enhanced images, and net contrast enhancement was calculated by subtracting the CT attenuation value in TNC images from those of corresponding contrast enhanced images.

### Statistical Analysis

All statistical analyses were performed using SPSS software (IBM SPSS Statistics ver. 19.0; IBM, Inc., Armonk, NY, USA). Continuous data are presented as the mean  $\pm$  standard deviation. Agreement in CT attenuation measurements between TNC and VNC images were analyzed by calculating the intraclass correlation coefficient (ICC) and using the Bland-Altman method. For visual assessment, the degree of agreement between TNC and VNC images for highly attenuating or calcified nodes was analyzed using

$\kappa$  statistics, as was the degree of agreement between independent observers. A partial correlation analysis was used to determine the relationships between value differences between TNC and VNC images, and both the CT attenuation in TNC and the net contrast enhancement. The analysis between the difference value and CT attenuation in TNC images was adjusted by the net contrast enhancement. In Cohen Kappa statistics,  $\kappa$  value was interpreted as follows: 0.8 to 1.0, very good; 0.6 to 0.8, good; 0.4 to 0.6, moderate; 0.2 to 0.4, fair; and 0.0 to 0.2, poor. The strength of correlation was determined using a scale as follows: 0.9 to 1.0 (correlation coefficient), very strong; 0.7 to 0.9, strong; 0.4 to 0.7, moderate; 0.2 to 0.4, weak; and 0.0 to 0.2, very weak. A *p* value of less than 0.05 was considered a significant difference, and all *p* values were two-tailed.

## RESULTS

A total of 112 nodes were assessed from 45 consecutive patients. The mean number of nodes included in each patient was  $2.5 \pm 1.1$  (range, 1-4).

The mean CTDI values were  $6.5 \pm 0.5$  mGy for single scan and  $5.4 \pm 0.9$  mGy for dual-energy scan. The mean DLP was  $191.9 \pm 56.6$  mGy·cm for TNC images and  $181.2 \pm 29.6$  mGy·cm for VNC images (*p* = 0.215).

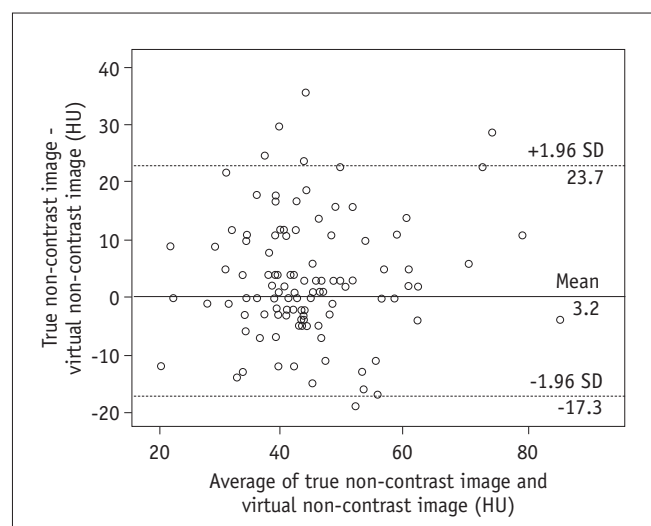


**Fig. 1. Results of Bland-Altman method.** True non-contrast image and virtual non-contrast image (mean difference, 3.2 HU; 95% CI: -17.3 HU, 23.7 HU). CI = confidence interval, HU = Hounsfield unit, SD = standard deviation

**Table 1. Visual Assessment of Mediastinal Nodal Groups in True Non-Contrast (TNC) and Virtual Non-Contrast (VNC) Images**

Visual Score* in TNC	Visual Score in VNC			Total
	0	1	2	
0	94 (83.9)	2 (1.8)	0	96 (85.7)
1	11 (9.8)	4 (3.6)	0	15 (13.4)
2	0	1 (0.9)	0	1 (0.9)
Total	105 (93.8)	7 (6.3)	0	112 (100)

**Note.**— Numbers in parentheses are percentages.\*Visual score: 0, CT attenuation of lymph node  $\leq$  aorta; 1, CT attenuation of lymph node  $>$  aorta; 2, calcification in lymph node

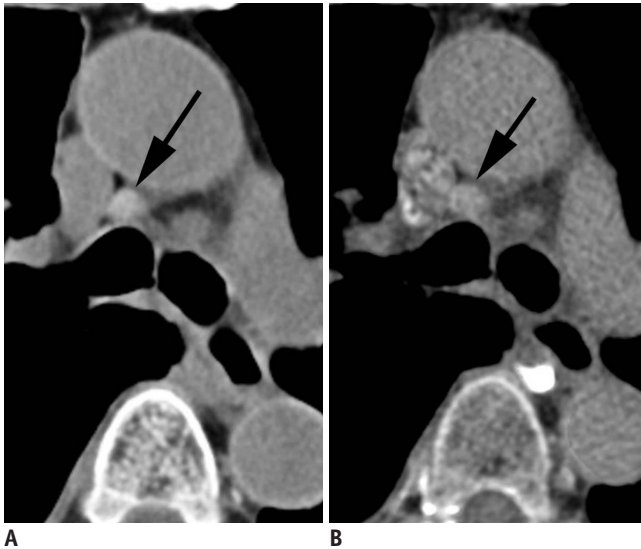


**Fig. 2. Lymph node with score of 1 in both true non-contrast (TNC) and virtual non-contrast (VNC) images.**  
Right lower paratracheal lymph node (arrow) shows higher attenuation than aorta in both TNC (A) and VNC (B) images.

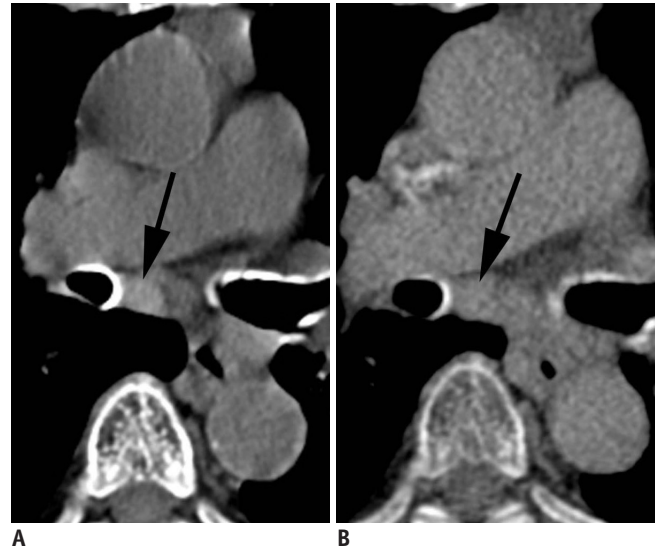


**Fig. 3. Lymph node with score of 1 in true non-contrast (TNC) image, but score of 0 in corresponding virtual non-contrast (VNC) image.**  
Subcarinal lymph node (arrow) shows attenuation greater than that of aorta in TNC image (A), but attenuation similar to that of aorta in VNC image (B).

### Comparison of the CT Attenuation on TNC and VNC Images

CT attenuation measurements were recorded from VNC and TNC images in each corresponding slice and region. The mean ROI area for TNC images was  $108.0 \pm 102.8 \text{ mm}^3$  (range, 21-600  $\text{mm}^3$ ) and  $107.6 \pm 102.5 \text{ mm}^3$  (range, 21-600  $\text{mm}^3$ ) for VNC images.

CT attenuations on TNC and VNC images showed moderate agreement (ICC, 0.612;  $p = 0.000$ ). Results of the Bland-Altman method for the agreement of CT attenuations in TNC and VNC images are shown in Figure 1. The mean difference in CT attenuation between TNC and VNC images was 3.2 HU (95% confidence interval: -17.3 HU, 23.7 HU).

The mean CT attenuation of nodes in TNC images was  $46.4 \pm 12.3 \text{ HU}$  (range, 15-89 HU) and  $43.2 \pm 11.6 \text{ HU}$  (range, 18-87 HU) in VNC images. The mean absolute difference between TNC and VNC images was  $7.8 \pm 7.6 \text{ HU}$  (range, 0-36 HU). The absolute difference was  $\leq 15 \text{ HU}$  in 82.1% (92/112) of nodes; and  $\leq 10 \text{ HU}$  in 65.2% (73/112) of nodes.

### Visual Assessment

The two investigators showed very good inter-observer agreement for the visual assessment of nodes in TNC images ( $\kappa$  value, 0.804) and good agreement in VNC images ( $\kappa$  value, 0.650).

The visual scores for nodes in TNC and VNC images showed fair agreement ( $\kappa$  value, 0.335). The numbers of nodes with scores of 0, 1, and 2 were 96, 15, and 1 in TNC images, and 105, 7, and 0 in VNC images, respectively (Table 1). Among the 15 nodes that were scored as 1 in TNC images, four of the same nodes were scored as 1 in the corresponding VNC images (Fig. 2); the remaining 11 nodes were downgraded to a score of 0 (Fig. 3). One node was scored as 2 in the TNC image set, but this extreme degree of attenuation due to calcification was not detected in the corresponding contrast-enhanced image; it was instead underscored as a 1 in the VNC image (Fig. 4).

**Factors Affecting Differences between TNC and VNC Images**

In general, nodes showing attenuation higher than the aorta in TNC images showed less attenuation in VNC images. The degree of CT attenuation in TNC images demonstrated a moderate positive correlation with differences between TNC

and VNC images (CT attenuation in TNC-CT attenuation in VNC) (partial correlation coefficient adjusted by net contrast enhancement, 0.455;  $p = 0.000$ ; Fig. 5A), suggesting that the CT attenuation in VNC images was much lower than in TNC images for nodes showing high attenuation or calcification.

Net contrast enhancement showed a weak negative correlation with the difference between TNC and VNC images (partial correlation coefficient adjusted by CT attenuation in TNC, -0.245;  $p = 0.010$ ; Fig. 5B), indicating that nodes with high net contrast enhancement had slightly higher CT attenuation in VNC than in TNC images.



**Fig. 4. Lymph node with score of 2 in true non-contrast (TNC) image and score of 1 in corresponding virtual non-contrast (VNC) image.**

Right lower paratracheal lymph node (arrow) shows punctate calcifications in TNC image (A), whereas it shows only diffuse high attenuation in VNC image (B). Note that calcifications in aortic arch and trachea are much smaller in VNC image than in TNC image.

**DISCUSSION**

Although CT has poor sensitivity and specificity for the detection of mediastinal node metastasis, calcification or CT attenuation higher than that of the great vessels is one of the most important deterministic findings of benignity of the mediastinal nodes in patients with malignancy. This is particularly important for mediastinal nodal staging in patients with NSCLC (1, 2, 6, 11). FDG-PET can potentially detect tumor activity in non-enlarged nodes and is now widely used for the staging of NSCLC, and it offers advantages over CT alone in assessing mediastinal nodes. However, FDG-PET has a high false-positive rate for mediastinal nodes, especially in regions where the

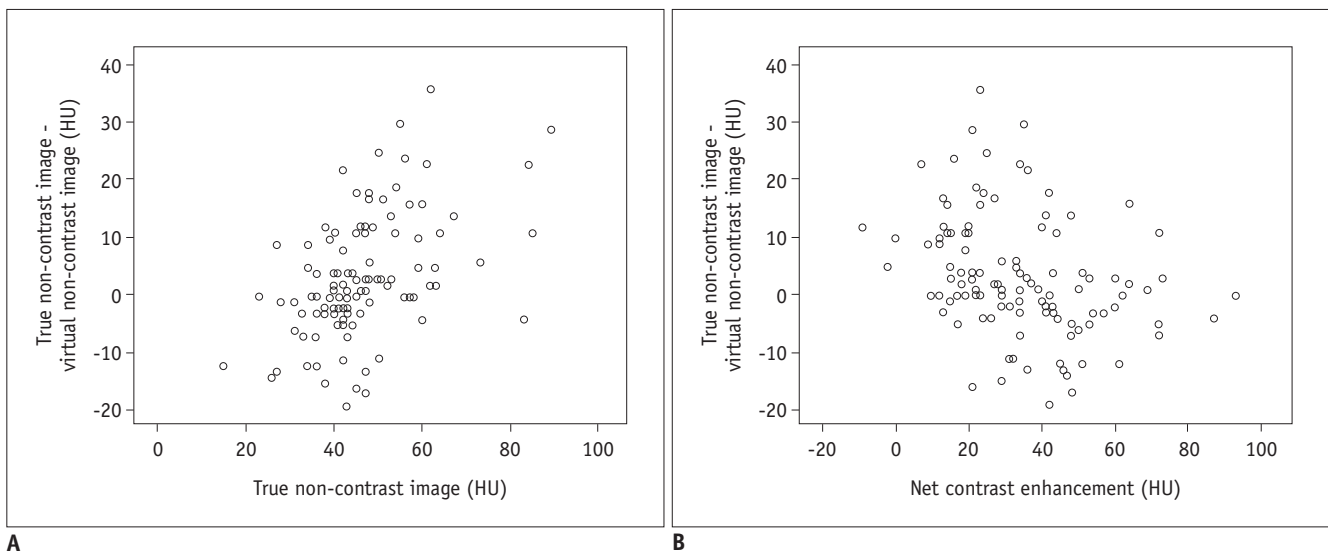


**Fig. 5. Relationships among difference between true non-contrast (TNC) and virtual non-contrast (VNC) images, CT attenuation in TNC images, and net contrast enhancement in assessment of mediastinal lymph nodes.**

A. TNC-VNC attenuation difference and CT attenuation in TNC images showed moderate positive correlation (partial correlation coefficient adjusted by net contrast enhancement, 0.455;  $p = 0.000$ ). B. TNC-VNC attenuation difference and net contrast enhancement demonstrated weak negative correlation (partial correlation coefficient adjusted by CT attenuation in TNC, -0.245;  $p = 0.010$ ). HU = Hounsfield unit

prevalence of inflammatory lung disease is high (2, 3, 6). Thus, based on FDG-PET alone, a patient may be denied potentially curative surgery if the mediastinal abnormality detected by FDG-PET is not further evaluated with an invasive mediastinal procedure.

Lymph nodes showing false positive FDG uptake have histopathologic characteristics that include anthracofibrosis, lymphoid follicular hyperplasia, and granulomatous infection, and may demonstrate calcification or CT attenuation greater than that caused by the great vessels on non-contrast CT images (1, 4-6). Li et al. (2) reported that nodes showing CT attenuation higher than that of the aorta were determined to be benign despite showing positive FDG uptake. This greatly improved the positive predictive value for mediastinal nodal diagnosis to 94.7%, compared to 65.5% when only FDG uptake was applied to determine nodal status. In the preoperative staging of NSCLC, Shim et al. (6) also reported that 35 of a total of 36 nodes which showed both FDG uptake and calcification or CT attenuation greater than that of the great vessels were benign. However, high CT attenuation in lymph nodes may not be detected on contrast-enhanced images alone (7), but instead may require an additional non-contrast scan that is usually excluded from routine chest CT protocol to prevent additional radiation exposure.

Dual energy CT scans may be generated by scanners using various types of techniques, including two tubes and two corresponding detector arrays (dual-source CT), kilovolt switching techniques, or the detector-level scintigraphic approach, in which energy discrimination occurs at the level of the detector (8). Dual-energy CT may be used to distinguish iodine from soft tissue due to their different K edge, which refers to the spike in attenuation that occurs at energy levels just greater than the K-shell binding energy, because of the increased photoelectric absorption at these energy levels. K edge values vary for each element, and they increase as the atomic number increases. In a previous study by Huda et al. (10), the mean photon energy was found to be 43.7 keV for an X-ray tube potential of 80 kV and 61.5 keV for 140 kV. Because the mean photon energy of 80 kV tube is close to the K edge of iodine (33.2 keV), the photoelectric absorption and thus the CT attenuation of iodine is substantially higher at 80 kV than it is at 140 kV, whereas those elements most prevalent in soft tissue have much lower K edge values (hydrogen, 0.01; carbon, 0.28; nitrogen, 0.40; oxygen, 0.53), with only slight differences in photoelectric absorption between 80 kV and 140 kV.

This substantial increase in the photoelectric absorption of iodine at 80 kV enables the subtraction of the iodine signal from dual-energy CT data and the generation of VNC images.

The clinical feasibility of using VNC rather than TNC images has been validated in the evaluation of solitary pulmonary nodules, renal and hepatic masses, aortic endoleak, and intracerebral bleeding (7, 12-15), but the reliability of VNC in the assessment of mediastinal lymph node has not been evaluated. Our study demonstrated that VNC images may provide information of high CT attenuation of nodes without obtaining additional non-contrast enhanced CT scan, although there was an underestimation of high CT attenuation or calcification in VNC images compared to TNC images. Five of 16 nodes, which showed high CT attenuation ( $n = 15$ ) or calcification ( $n = 1$ ) in TNC images but did not demonstrate calcification in contrast-enhanced images, revealed high CT attenuation in VNC images.

Underestimation of calcification in VNC images has been reported in previous studies (7, 12). De Cecco et al. (12) demonstrated erroneous aortic calcification subtraction in VNC images of the liver, while Chae et al. (7) revealed that the sizes of calcifications in a solitary pulmonary nodule or mediastinal lymph nodes were smaller in VNC images than in corresponding TNC images. In this study, nodes that showed attenuation higher than that of the aorta in TNC images demonstrated a decrease in CT attenuation in corresponding VNC images. This discrepancy was attributed to errors in post-processing due to the increased presence of calcification and anthracotic pigmentation in strongly attenuating nodes. Calcium shows larger differences in photoelectric absorption between 80 kV and 140 kV compared to soft tissue, because its K edge (4.0 keV) is closer to 80 kV than that of soft tissue, resulting in the partial subtraction of the calcium signal while generating the VNC image. Similarly, the presence of anthracotic pigmentation, which was revealed upon histopathologic examination to be present in most lymph nodes showing strong CT attenuation, may also lead to a subtraction error in post-processing. In addition to these errors, artifacts related to the incomplete subtraction of the contrast medium may also occur in the greater vessels or highly vascular organs, such as the spleen (12, 16). Inhomogeneous high attenuation in the superior vena cava is frequently observed in VNC images when the highly concentrated contrast medium remains in the vena cava. In this study, a weak correlation was observed between the

net contrast enhancement and increased CT attenuation in VNC images. The higher net contrast enhancement means that the higher portion of incomplete iodine subtraction leads to an increase in CT attenuation in VNC images. However, based on the result of our study, in which the relationship between the net contrast enhancement and the difference (TNC-VNC) showed lower correlation strength than that between the CT attenuation of nodes in TNC and the difference, this effect seems to be much less than the effect of partial subtraction of calcium, or the presumed anthracotic pigments, in calculating VNC images of lymph nodes. Thus, VNC images created with the presently available post-processing techniques are not always equivalent to TNC images.

Our study has several limitations. First, the number of nodes showing visual scores of 1 or 2 was small (16/112 in TNC images), which may be because the study included only those nodes that were > 1 cm in short diameter. Most nodes that show false positive FDG uptake and high CT attenuation are small, usually < 1 cm in size (4). We did not include such small nodes because the measurement of CT attenuation may then be more strongly influenced by partial volume artifacts. In fact, had we included small high-attenuation nodes, the discrepancy between TNC and VNC images would have been more apparent. Another limitation is that the calculation of VNC depends on post-processing algorithms. Post-processing software that is more effective in subtracting the iodine and calcium signals may provide VNC images that are more equivalent to TNC images; and with further validation, may replace TNC images even in the more complicated assessment of mediastinal nodes.

To the best of our knowledge, this is the first study that has evaluated the reliability of VNC images in the assessment of mediastinal lymph node. Further study will be needed with newer dual energy CT scanners or post-processing software which may provide reliable VNC images for lymph node evaluation.

In conclusion, VNC images may be useful in the evaluation of mediastinal lymph nodes by providing additional information of high CT attenuation of nodes, although it is underestimated compared to TNC images.

## REFERENCES

- Kim YK, Lee KS, Kim BT, Choi JY, Kim H, Kwon OJ, et al. Mediastinal nodal staging of nonsmall cell lung cancer using integrated 18F-FDG PET/CT in a tuberculosis-endemic country: diagnostic efficacy in 674 patients. *Cancer* 2007;109:1068-1077
- Li M, Wu N, Liu Y, Zheng R, Liang Y, Zhang W, et al. Regional nodal staging with 18F-FDG PET-CT in non-small cell lung cancer: additional diagnostic value of CT attenuation and dual-time-point imaging. *Eur J Radiol* 2012;81:1886-1890
- Liao CY, Chen JH, Liang JA, Yeh JJ, Kao CH. Meta-analysis study of lymph node staging by 18 F-FDG PET/CT scan in non-small cell lung cancer: comparison of TB and non-TB endemic regions. *Eur J Radiol* 2012;81:3518-3523
- Toba H, Kondo K, Otsuka H, Takizawa H, Kenzaki K, Sakiyama S, et al. Diagnosis of the presence of lymph node metastasis and decision of operative indication using fluorodeoxyglucose-positron emission tomography and computed tomography in patients with primary lung cancer. *J Med Invest* 2010;57:305-313
- Iskender I, Kadioglu SZ, Cosgun T, Kapicibasi HO, Sagioglu G, Kosar A, et al. False-positivity of mediastinal lymph nodes has negative effect on survival in potentially resectable non-small cell lung cancer. *Eur J Cardiothorac Surg* 2012;41:874-879
- Shim SS, Lee KS, Kim BT, Chung MJ, Lee EJ, Han J, et al. Non-small cell lung cancer: prospective comparison of integrated FDG PET/CT and CT alone for preoperative staging. *Radiology* 2005;236:1011-1019
- Chae EJ, Song JW, Seo JB, Krauss B, Jang YM, Song KS. Clinical utility of dual-energy CT in the evaluation of solitary pulmonary nodules: initial experience. *Radiology* 2008;249:671-681
- Coursey CA, Nelson RC, Boll DT, Paulson EK, Ho LM, Neville AM, et al. Dual-energy multidetector CT: how does it work, what can it tell us, and when can we use it in abdominopelvic imaging? *Radiographics* 2010;30:1037-1055
- Kang MJ, Park CM, Lee CH, Goo JM, Lee HJ. Dual-energy CT: clinical applications in various pulmonary diseases. *Radiographics* 2010;30:685-698
- Huda W, Scalzetti EM, Levin G. Technique factors and image quality as functions of patient weight at abdominal CT. *Radiology* 2000;217:430-435
- Darling GE, Maziak DE, Inculet RI, Gulenchyn KY, Driedger AA, Ung YC, et al. Positron emission tomography-computed tomography compared with invasive mediastinal staging in non-small cell lung cancer: results of mediastinal staging in the early lung positron emission tomography trial. *J Thorac Oncol* 2011;6:1367-1372
- De Cecco CN, Buffa V, Fedeli S, Luzzi M, Vallone A, Ruopoli R, et al. Dual energy CT (DECT) of the liver: conventional versus virtual unenhanced images. *Eur Radiol* 2010;20:2870-2875
- Chandarana H, Godoy MC, Vlahos I, Graser A, Babb J, Leidecker C, et al. Abdominal aorta: evaluation with dual-source dual-energy multidetector CT after endovascular repair of aneurysms--initial observations. *Radiology* 2008;249:692-700
- Graser A, Johnson TR, Hecht EM, Becker CR, Leidecker C, Staehler M, et al. Dual-energy CT in patients suspected of

- having renal masses: can virtual nonenhanced images replace true nonenhanced images? *Radiology* 2009;252:433-440
15. Stolzmann P, Frauenfelder T, Pfammatter T, Peter N, Scheffel H, Lachat M, et al. Endoleaks after endovascular abdominal aortic aneurysm repair: detection with dual-energy dual-source CT. *Radiology* 2008;249:682-691
16. Toepker M, Moritz T, Krauss B, Weber M, Euller G, Mang T, et al. Virtual non-contrast in second-generation, dual-energy computed tomography: reliability of attenuation values. *Eur J Radiol* 2012;81:e398-e405